



THE UNIVERSITY *of* EDINBURGH

## Edinburgh Research Explorer

### A framework for estimating forest disturbance intensity from successive remotely sensed biomass maps

**Citation for published version:**

Hill, TC, Ryan, CM & Williams, M 2015, 'A framework for estimating forest disturbance intensity from successive remotely sensed biomass maps: Moving beyond average biomass loss estimates', *Carbon Balance and Management*, vol. 10, no. 1, 27. <https://doi.org/10.1186/s13021-015-0039-0>

**Digital Object Identifier (DOI):**

[10.1186/s13021-015-0039-0](https://doi.org/10.1186/s13021-015-0039-0)

**Link:**

[Link to publication record in Edinburgh Research Explorer](#)

**Document Version:**

Publisher's PDF, also known as Version of record

**Published In:**

Carbon Balance and Management

**Publisher Rights Statement:**

© 2015 Hill et al.

Open Access This article is distributed under the terms of the Creative Commons Attribution 4.0 International License (<http://creativecommons.org/licenses/by/4.0/>), which permits unrestricted use, distribution, and reproduction in any medium, provided you give appropriate credit to the original author(s) and the source, provide a link to the Creative Commons license, and indicate if changes were made.

**General rights**

Copyright for the publications made accessible via the Edinburgh Research Explorer is retained by the author(s) and / or other copyright owners and it is a condition of accessing these publications that users recognise and abide by the legal requirements associated with these rights.

**Take down policy**

The University of Edinburgh has made every reasonable effort to ensure that Edinburgh Research Explorer content complies with UK legislation. If you believe that the public display of this file breaches copyright please contact [openaccess@ed.ac.uk](mailto:openaccess@ed.ac.uk) providing details, and we will remove access to the work immediately and investigate your claim.



METHODOLOGY

Open Access



# A framework for estimating forest disturbance intensity from successive remotely sensed biomass maps: moving beyond average biomass loss estimates

T. C. Hill<sup>1,2,3\*</sup>, C. M. Ryan<sup>2</sup> and M. Williams<sup>2,3</sup>

## Abstract

**Background:** The success of satellites in mapping deforestation has been invaluable for improving our understanding of the impacts and nature of land cover change and carbon balance. However, current satellite approaches struggle to quantify the intensity of forest disturbance, i.e. whether the average rate of biomass loss for a region arises from heavy disturbance focused in a few locations, or the less severe disturbance of a wider area. The ability to distinguish between these, very different, disturbance regimes remains critical for forest managers and ecologists.

**Results:** We put forward a framework for describing all intensities of forest disturbance, from deforestation, to widespread low intensity disturbance. By grouping satellite observations into ensembles with a common disturbance regime, the framework is able to mitigate the impacts of poor signal-to-noise ratio that limits current satellite observations. Using an observation system simulation experiment we demonstrate that the framework can be applied to provide estimates of the mean biomass loss rate, as well as distinguish the intensity of the disturbance. The approach is robust despite the large random and systematic errors typical of biomass maps derived from radar. The best accuracies are achieved with ensembles of  $\geq 1600$  pixels ( $\geq 1 \text{ km}^2$  with 25 by 25 m pixels).

**Summary:** The framework we describe provides a novel way to describe and quantify the intensity of forest disturbance, which could help to provide information on the causes of both natural and anthropogenic forest loss—such information is vital for effective forest and climate policy formulation.

**Keywords:** Deforestation, Forest, Degradation, Disturbance, Intensity, Biomass, REDD, Satellite, Remote sensing, Carbon

## Background

Tropical deforestation has been estimated to occur at a rate of 13 million ha per year [1], with an associated net loss of forest biomass of  $1.3 \pm 0.7 \text{ Pg C year}^{-1}$  [2]. Remote sensing has been successful at mapping global deforestation [3, 4]. However, deforestation presents a simplified view of forest disturbance that ignores the many gradations of lower intensity, but often widespread, forest disturbance and degradation [5]. Forest disturbance refers

to the mechanisms which limit biomass by causing its destruction [6]. The impact of forest disturbance is highly variable, leading to the total or partial loss of biomass through a diverse range of natural (e.g. disease, droughts, fires, herbivory and windstorms) and/or anthropogenic processes (e.g. urbanisation, agriculture, selective logging, and fires). Remotely sensed information on the spatial extent and intensity of forest disturbance would be extremely useful for managers and ecologists in attempts to develop a mechanistic understanding of forest degradation and the processes of forest disturbance [7, 8].

Unfortunately, whilst satellites have the coverage to provide global information on forest disturbance, very

\*Correspondence: t.c.hill@exeter.ac.uk

<sup>1</sup> Department of Earth and Environmental Science, University of St Andrews, Irvine Building, North Street, St Andrews, UK

Full list of author information is available at the end of the article

few studies have attempted to do so [9]. The focus of remote sensing has remained on mapping deforestation (e.g. [3]) and arises from a number of technological limitations which include, amongst other factors, observation precision and the relative “directness” of the observation [10–12]. Ideally remote sensing measurements would have a direct dependence on the quantity being estimated; however current optical satellite derived estimates of forest disturbance are not able to achieve this ideal. Instead, optical satellite measurements of forest disturbance rely on observing physical properties that are expected to correlate with disturbance (e.g. changes in leaf area that can be detected by satellites due to a change in the absorption in the chlorophyll spectral bands). When these correlations change, indirect measures cannot be expected to provide a robust estimate of disturbance.

As Synthetic aperture radar (SAR) is sensitive to the structural properties of forests it can be thought of as a more direct measure of forest biomass than the passive optical alternatives [8, 13, 14]. SAR provides one of the only viable data sources currently available for global monitoring of forest disturbance at moderate spatial resolutions. However, the low signal to noise ratio of SAR leads to poor precision and large uncertainty in the estimated biomass of individual pixels [13] and this equates to high levels of uncertainty when detecting biomass change at the pixel level. Filtering can be used to improve the signal to noise ratio of SAR, but this improvement comes at the expense of a reduction in the effective spatial resolution of the biomass change estimates. Therefore remote sensing can provide regional estimates of biomass change or fine scale maps of deforestation, but it cannot yet be said to truly determine the intensity of forest degradation across scales [13].

In this study we set out a novel framework for quantifying the intensity of forest disturbance from successive remotely sensed biomass maps. This approach can describe both focused high intensity forest loss and low intensity, widespread degradation. We provide an example methodology to exploit this framework using SAR data with realistic observation errors. We explore the strengths and limitations of this approach using an observation system simulation experiment.

## Results and discussion

### A framework for quantifying the intensity of forest disturbance

The framework that we propose describes forest disturbance for an area in which all satellite observation pixels are assumed to experience the same disturbance regime. That is, whilst each pixel might or might not be disturbed, each pixel within each area has the same probability of

being disturbed and the same relative loss of biomass when disturbed. We consider an ensemble of  $n$  remote sensing pixels, which are observed on two successive dates ( $t = 1$  and  $t = 2$ ). This approach builds on an earlier framework set out in Williams [15] that used the biomass distribution at a single point in time. The first advantage of this new approach is that it allows ensemble statistics to be calculated, negating the limitations of poor signal to noise of individual biomass pixels by estimating ensemble’s mean fractional loss of biomass per year ( $E_M$ ). The second advantage of the framework is that it permits  $E_M$  to be split into two factors for the ensemble: the probability of disturbance per year for each ensemble pixel member ( $E_P$ ) and the fractional loss of biomass per disturbance for each disturbed ensemble pixel member ( $E_I$ ), Eq. 1.

$$E_M \approx E_P E_I \quad (1)$$

Both  $E_M$  and its factors  $E_P$  and  $E_I$  can take values ranging from 0–1. Where, for example, an  $E_P = 0.05$  would imply a 1 in 20 chance of each pixel being disturbed in a year. An  $E_I = 0.2$  implies that, if disturbed, a pixel will lose 20 % of its biomass. Combining these example factors would lead to the expectation of  $E_M = 0.01$ , or a 1 % reduction in mean biomass for the ensemble. The ensemble size can be picked to balance the competing requirements of high precision on estimates of  $E_M$ ,  $E_P$  and  $E_I$  and meeting the assumption of a continuous disturbance regime.

The inclusion of the factors  $E_P$  and  $E_I$  allows a flexible description of biomass loss, without the arbitrary distinction between deforestation and lower intensity forest disturbance. Forest disturbance (other than deforestation) can be represented by the parameter space  $0 < E_M < 1$ ,  $0 < E_I < 1$  and  $0 < E_P \leq 1$  (Fig. 1). There are also several special cases: the total deforestation of the ensemble area ( $E_M = 1$ ,  $E_I = 1$  and  $E_P = 1$ ); partial deforestation within the area ( $0 < E_M < 1$ ,  $E_I = 1$  and  $0 < E_P < 1$ ); and no disturbance ( $E_M = 0$ ).

Describing forest disturbance using this framework has a number of advantages over traditional descriptors as it avoids the need for an arbitrary threshold for a forest cover loss used in other studies, e.g. [16]. In turn, this allows for a more nuanced description of forest disturbance than is possible with categorical land cover classes, or measures of forest cover.

### Using the framework to estimate biomass loss and disturbance intensity

Using the disturbance framework, our observation system simulation experiments (OSSE) show it is possible to robustly estimate the mean biomass loss for the ensemble ( $E_M$ ) and also the disturbance regime, as described by

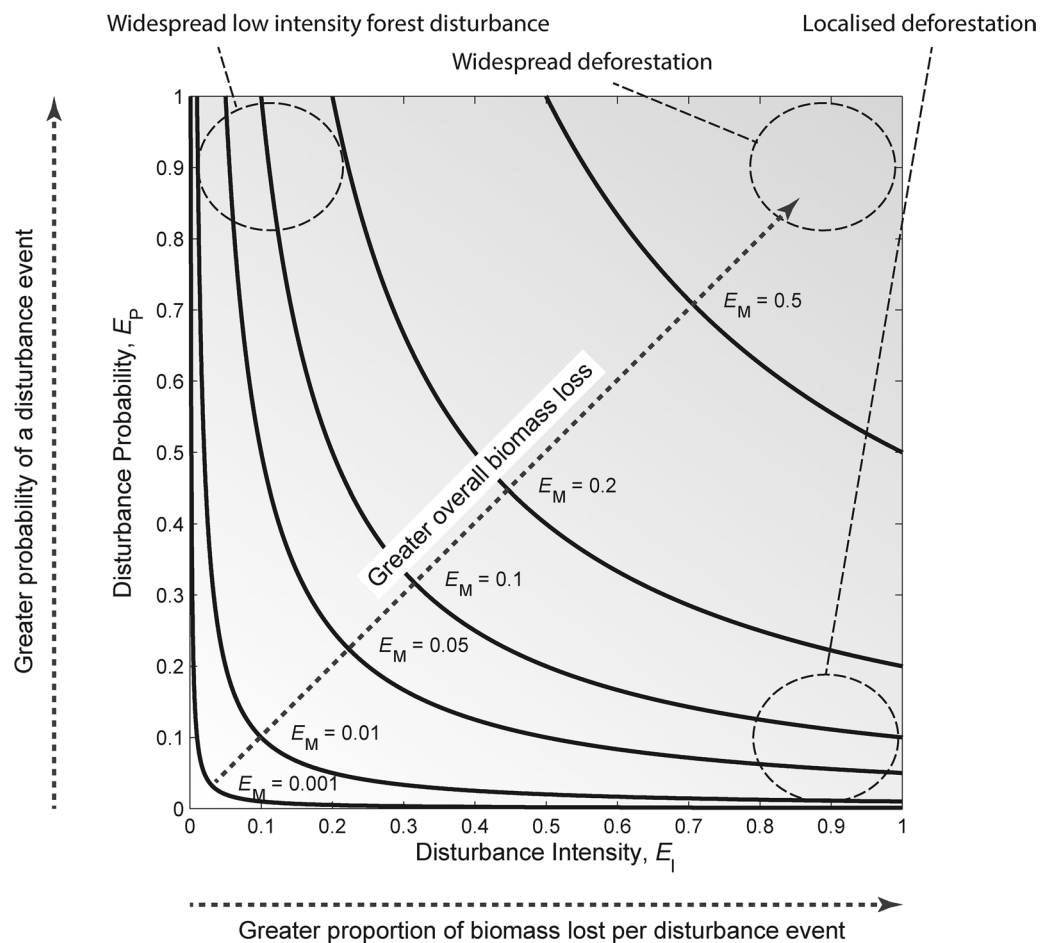


**Fig. 1** The relationships between the magnitude of disturbance (i.e. the mean fractional disturbance of a region per year,  $E_M$ ), the disturbance probability (i.e. the probability of a pixel being disturbed each year,  $E_P$ ), and the disturbance intensity (i.e. the fraction of biomass lost if disturbed,  $E_I$ ) are shown. Indicated within the figure are regions corresponding to widespread forest degradation, localised deforestation and widespread deforestation

$E_P$  and  $E_I$  (Fig. 2; Table 1).  $E_M$  is better constrained than either  $E_I$  or  $E_P$ , reflecting the direct impact of  $E_M$  on the mean of the biomass distribution versus the more variable impacts of the  $E_I$  or  $E_P$  on the second and third order moments: standard deviation and skew. With larger mean disturbances the constraints on  $E_I$  or  $E_P$  improve, presumably due to the larger number of pixels effected and/or greater impact on the observed biomass.

#### How the framework is affected by observation bias

It is highly likely that biomass maps used with the framework will not only have random noise, but also systematic observation errors [13], therefore we test the framework's sensitivity to bias. The inclusion of a realistic observation bias of  $\pm 160 \text{ gC m}^{-2}$  ( $\pm 1.6 \text{ tC ha}^{-1}$ ) [13] had the largest impacts on the estimates of  $E_M$ , which showed a bias of 0.004 (0.4 %). However  $E_I$  and  $E_P$  were less affected

(Fig. 3; Table 1) and it was still possible to distinguish high and low intensity disturbance regimes. The bias in the estimate for  $E_M$  is consistent with change in the mean biomass that is implied by a bias of  $160 \text{ gC m}^{-2}$ , and would therefore apply to any other approach to estimating biomass loss.

#### What is the optimal ensemble size?

The accuracy of predictions using the framework are best when considering an ensemble size of  $n \geq 1600$ , whilst for  $n \leq 400$ , the precision of our estimates drops rapidly (Fig. 4; Table 1). Therefore, for the 25 m pixels typical of current SAR biomass estimates, the recommended ensemble size covers an area of at least  $1 \text{ km}^2$  or 100 ha. The implication is that it must be reasonable to assume that the disturbance regime is constant across areas of at least 100 ha. We expect this minimum area to be

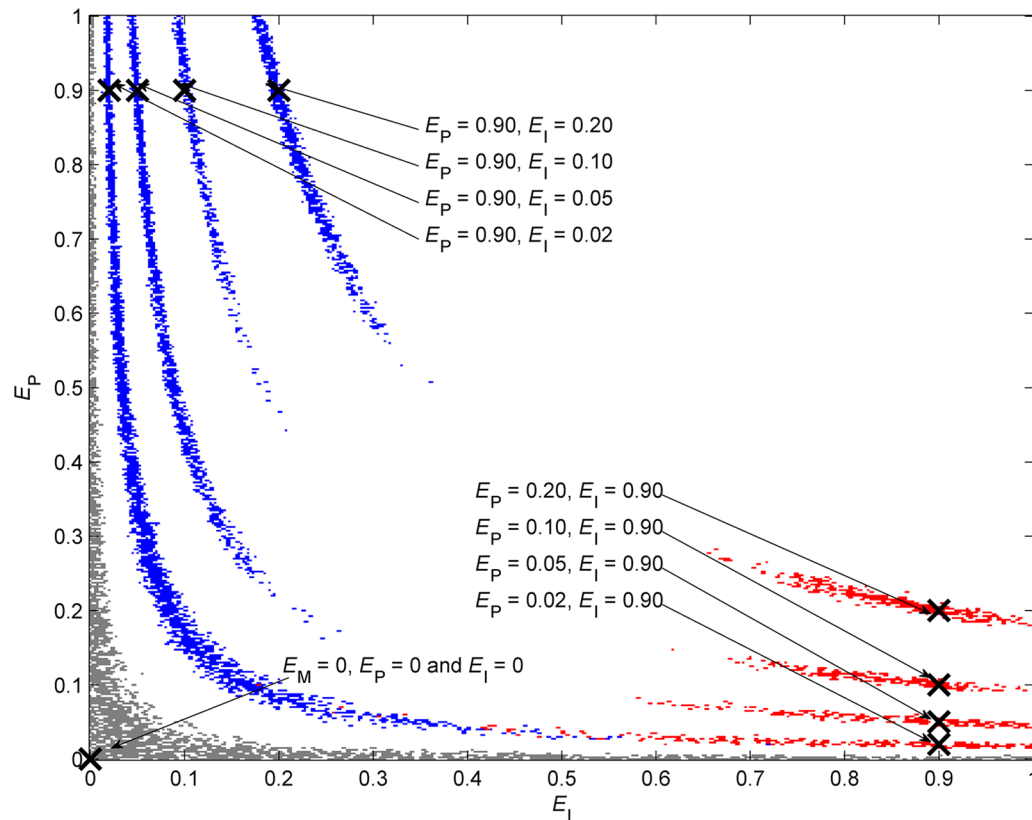


**Fig. 2** Estimates from the biomass difference approach for nine different combinations of disturbance intensity and disturbance probability. Crosses indicate the actual  $E_P$  and  $E_I$  used for each synthetic analysis. Coloured areas indicate the most likely combinations of  $E_I$  and  $E_P$  as estimated by the difference approach. The filled areas encompass the first 95 % of the cumulative likelihood,  $L$ . Low intensity cases are shown in blue, high intensity cases are shown in red and the special case of no disturbance is shown in grey

robust, at least for ALOS PALSAR data, but the sensitivity to ensemble size should be checked in each new study. It is worth noting that there is no requirement for these areas to be rectangular, or even contiguous. The grainy texture evident in the estimates from the analyses is due to the simulation of stochastic disturbances (Figs. 2, 3, 4). This graining is reduced with increasing ensemble size, but can be further reduced, at significant computational expense, by averaging repeat runs of the maximum likelihood estimation.

#### Alternative formulations of the framework

We formulated the framework in terms of a fractional change in biomass for both  $E_M$  and  $E_I$ . This is not the only possible formulation, nor is it necessarily the optimal for all situations; however, it is a mathematically simple approach to maintaining a positive (i.e. plausible) biomass for each pixel. The implicit assumptions of the formulation are: 1) that all pixels are equally likely to be disturbed, and 2) that when disturbed a fixed fraction is lost, irrespective of the starting biomass. It is possible to imagine scenarios that would not be well described

by our scheme where (say) selective logging only targets the largest trees (i.e.  $E_P$  is high for pixels above a threshold biomass and zero for all others). These scenarios do not contradict our first assumption of common disturbance regime for the ensemble and it should be possible to restate the parameters used in the framework to accommodate a particular set of assumptions about the disturbance regime. However the inclusion of more complicated mathematical representations and, specifically, more parameters, can be expected to increase the challenge of estimating the parameters of any new framework formulation and decrease its general applicability.

#### Limitations to the framework

Finally there are two notable caveats: Firstly, the success of the approach is strongly tied to the ability to characterise the random error of biomass estimates. The design of the analysis mitigates some of the errors as biomass errors that are consistent between the two biomass maps will be removed by this differencing. Whilst Ryan et al. (2012) report normal errors in the biomass domain, other studies assume errors will actually be normal in

**Table 1 The maximum (97.5 % CI), minimum (2.5 % CI) and 95 % CI range (maximum–minimum) for estimates of  $E_M$ ,  $E_I$  and  $E_P$  are shown for each of the test**

Figs.	Description	Ensemble size ( <i>n</i> )	Actual $E_I$	Actual $E_P$	Actual $E_M$	Est. $E_I$ (max/min/ range)	Est. $E_P$ (max/min/ range)	Est. $E_M$ (max/min/ range)
2	High intensity	1600	0.9	0.02	0.018	1.000/0.178/0.823	0.100/0.015/0.085	0.023/0.012/0.011
2	High intensity	1600	0.9	0.05	0.045	1.000/0.580/0.420	0.083/0.043/0.040	0.053/0.040/0.013
2	High intensity	1600	0.9	0.1	0.090	0.993/0.618/0.375	0.148/0.093/0.055	0.097/0.084/0.014
2	High intensity	1600	0.9	0.2	0.180	0.998/0.655/0.343	0.283/0.180/0.103	0.195/0.168/0.027
2	Low intensity	1600	0.02	0.9	0.018	0.720/0.013/0.708	1.000/0.020/0.980	0.023/0.011/0.012
2	Low intensity	1600	0.05	0.9	0.045	0.265/0.040/0.225	1.000/0.163/0.838	0.050/0.038/0.012
2	Low intensity	1600	0.1	0.9	0.090	0.208/0.088/0.120	1.000/0.443/0.558	0.100/0.086/0.014
2	Low intensity	1600	0.2	0.9	0.180	0.363/0.173/0.190	1.000/0.508/0.493	0.188/0.168/0.020
2	No disturbance	1600	0	0	0.000	1.000/0.000/1.000	1.000/0.000/1.000	0.006/0.000/0.006
3	High intensity: Bias = 160 gC m <sup>-2</sup>	1600	0.9	0.05	0.045	1.000/0.653/0.348	0.060/0.038/0.023	0.043/0.035/0.008
3	High intensity: Bias = 0 gC m <sup>-2</sup>	1600	0.9	0.05	0.045	1.000/0.468/0.533	0.098/0.038/0.060	0.049/0.035/0.014
3	High intensity: Bias = -160 gC m <sup>-2</sup>	1600	0.9	0.05	0.045	1.000/0.518/0.483	0.108/0.050/0.058	0.060/0.049/0.011
3	Low intensity: Bias = 160 gC m <sup>-2</sup>	1600	0.05	0.9	0.045	0.188/0.035/0.153	1.000/0.215/0.785	0.044/0.032/0.012
3	Low intensity: Bias = 0 gC m <sup>-2</sup>	1600	0.05	0.9	0.045	0.325/0.040/0.285	1.000/0.148/0.853	0.052/0.039/0.012
3	Low intensity: Bias = -160 gC m <sup>-2</sup>	1600	0.05	0.9	0.045	0.283/0.048/0.235	1.000/0.173/0.828	0.059/0.046/0.012
4	Area = 2000 by 2000 m	6400	0.05	0.9	0.045	0.128/0.045/0.083	1.000/0.350/0.650	0.048/0.042/0.006
4	Area = 1000 by 1000 m	1600	0.05	0.9	0.045	0.298/0.043/0.255	1.000/0.150/0.850	0.053/0.041/0.013
4	Area = 500 by 500 m	400	0.05	0.9	0.045	0.848/0.040/0.808	1.000/0.045/0.955	0.061/0.033/0.028
4	Area = 250 by 250 m	100	0.05	0.9	0.045	0.980/0.023/0.958	1.000/0.028/0.973	0.074/0.019/0.055

The 95 % CI range is expected encompass the actual  $E_M$ ,  $E_I$  and  $E_P$  used to generate the synthetic observations

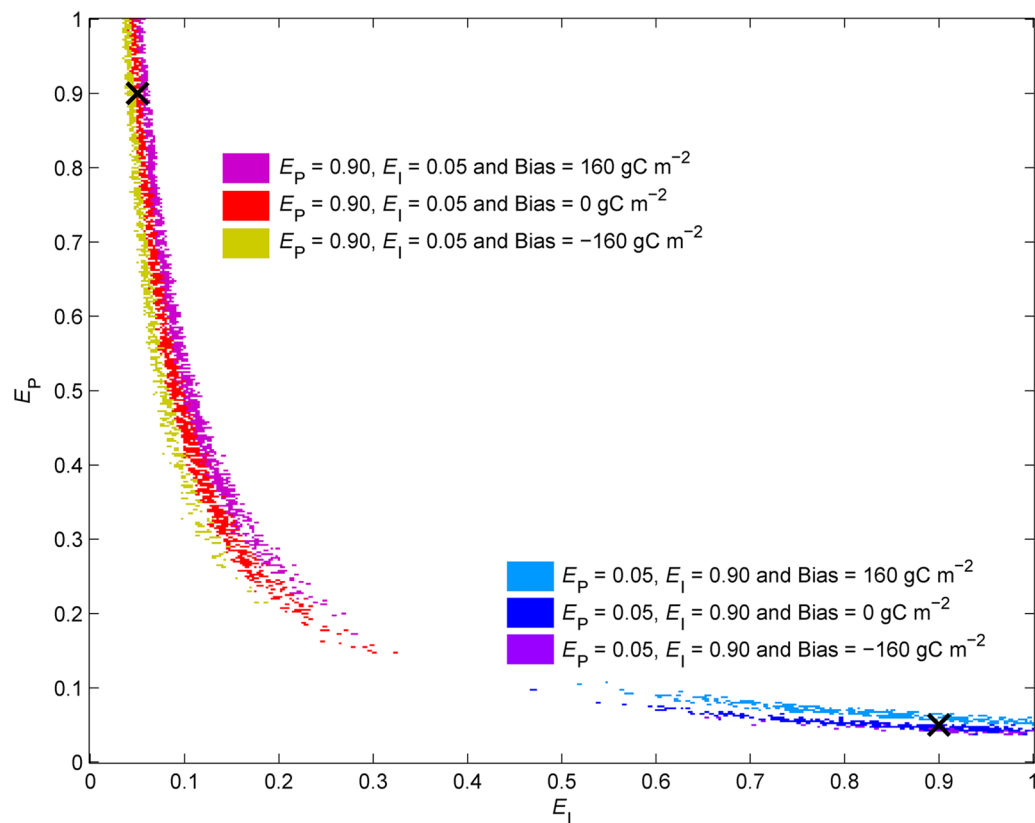


**Fig. 3** As for Fig. 2, but showing the impact of observation bias on estimated  $E_p$  and  $E_i$ . Biases of 160, 0 and  $-160 \text{ gC m}^{-2}$  are applied to the first of the biomass images. For each bias two example cases with the same  $E_M$  are shown: (1) High intensity disturbance,  $E_i = 0.9$  and  $E_p = 0.05$ . (2) Low intensity disturbance,  $E_i = 0.05$  and  $E_p = 0.9$

the dB (i.e.  $\log_{10}$ ) domain [17] which would result in log-normal, asymmetric errors on biomass estimates. We therefore reran the synthetic experiments with 0.5 dB error and achieved similar results. The second caveat is that the biomass differencing approach assumes the carbon model (A-DALEC) is unbiased. This assumption is, by definition, valid in a observation system simulation experiment (OSSE). However in practice the productivity of the ecosystem is not known perfectly, and so estimates of  $E_M$  can be expected to be biased. However the assumption is not as crude as it at first might seem: ignoring the production term (as is implicitly done by most deforestation algorithms) makes the assumption that the forest otherwise in steady state. This issue is likely to be more severe in field sites where less information is available on which to provide independent estimate of the rates of aboveground biomass accumulation, e.g. [18].

## Conclusions

From a management and policy perspective it is important to be able to distinguish between the different intensities of biomass loss as they may be associated with

different disturbances mechanisms (e.g. low intensity disturbances are likely driven by a need for timber or fuel, and high intensity disturbances driven by a need for agricultural land) [19]. However, current estimates of deforestation and biomass loss are not adequate for estimating lower intensity forest disturbance. Theoretically, high resolution biomass loss estimates could provide fine-scale estimates of forest degradation, but the current precision is not adequate and there is no immediate prospect of this changing, partly due to the speckle and other noise in SAR imagery [20]. The framework that we have described is a pragmatic representation of forest degradation that uses ensemble statistics to mitigate the poor precision of current SAR biomass estimates [13, 17, 20]. SAR is expected to remain a key technique for global mapping of forest biomass, and the framework we propose is compatible with the upcoming BIOMASS and new L-band satellites [14]. Using an OSSE we have shown that is possible to robustly estimate the parameters of the framework to describe forest disturbance, provided that two successive biomass maps, separated by at least one year, are available. We suggest that using



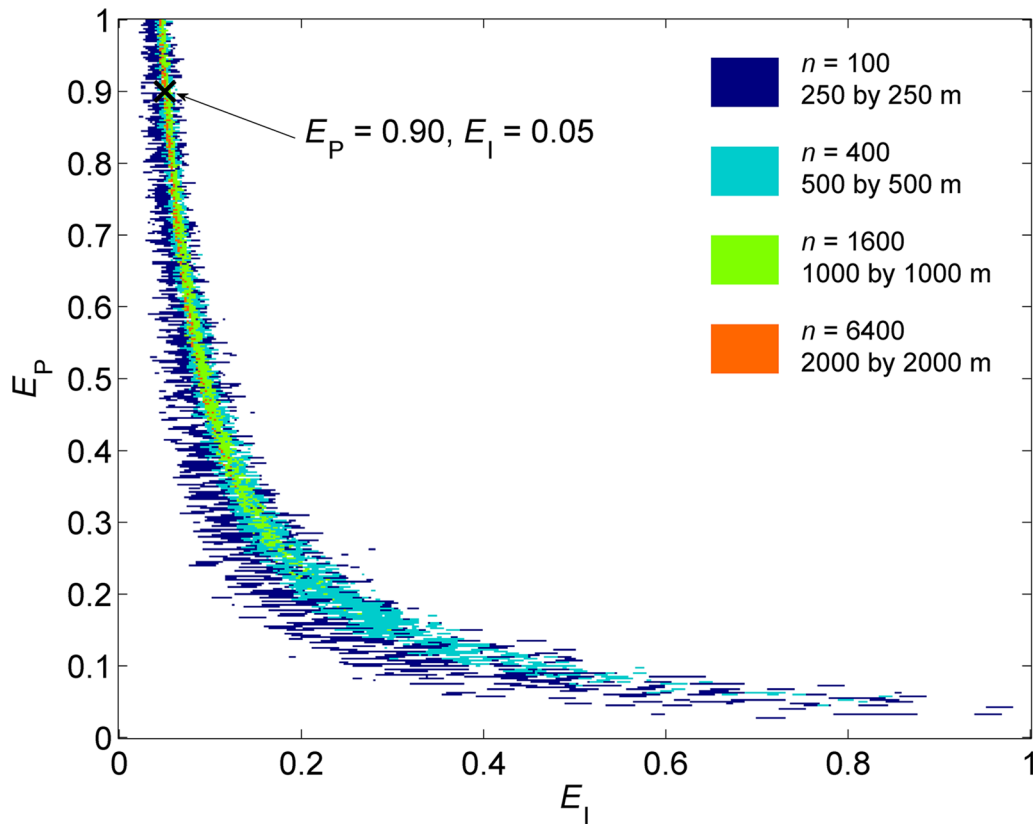


**Fig. 4** The effect of ensemble size (the number of pixels) on the analysis. The cross shows the synthetic truth and the coloured areas indicate the most likely  $E_I$  and  $E_P$

a similar framework will allow remote sensing studies to provide more relevant constraints on estimates of land-use change.

## Methods

### Estimating the framework parameters

A number of approaches could be taken to estimating  $E_M$ ,  $E_I$  and  $E_P$ , we chose to use maximum likelihood estimation. We identify the combinations of  $E_I$  and  $E_P$  that allow a simulations to most closely match the observed changes in the biomass distribution from time  $t = 1$  to time  $t = 2$ , for an ensemble of  $n$  pixels.

The observed biomass ( $O_i^t$ ) of the  $i$ th pixel at time  $t$  is sum of the actual biomass ( $B_i^t$ ) and the measurement noise ( $N_i^t$ ), Eq. 2. The observed biomass at time  $t + 1$ , follows the same logic (Eq. 3). The actual biomasses are related via the growth  $G_i^t$  and disturbance  $D_i^t$  of each pixel in the ensemble (Eq. 4).

$$O_i^t = B_i^t + N_i^t \quad \text{for } i = 1, 2, 3, \dots, n \quad (2)$$

$$O_i^{t+1} = B_i^{t+1} + N_i^{t+1} \quad \text{for } i = 1, 2, 3, \dots, n \quad (3)$$

$$B_i^{t+1} = B_i^t + G_i^t - D_i^t \quad \text{for } i = 1, 2, 3, \dots, n \quad (4)$$

Similarly we are able to simulate the observed biomass at time  $t$  ( $O_i^t$ ) based on the simulation biomass ( $B_i^t$ ) added to the simulated noise ( $N_i^t$ ), Eq. 5. The observed biomass at time  $t$  ( $O_i^{t+1}$ ) is calculated from the simulation biomass ( $B_i^t$ ) through the sum of the simulated growth ( $G_i^t$ ), the simulated disturbance ( $D_i^t$ ), and the simulated noise ( $N_i^{t+1}$ ), Eq. 6.

$$O_i^t = B_i^t + N_i^t \quad \text{for } i = 1, 2, 3, \dots, n \quad (5)$$

$$O_i^{t+1} = B_i^t + G_i^t - D_i^t + N_i^{t+1} \quad \text{for } i = 1, 2, 3, \dots, n \quad (6)$$

where  $D_i^t$  is related to the disturbance parameters in Eq. 7.

$$D_i^t = \begin{cases} 0 & \text{if } U([0, 1]) \geq E_P \\ E_I B_i^t & \text{otherwise} \end{cases} \quad \text{for } i = 1, 2, 3, \dots, n \quad (7)$$

We model  $G_i^t$  using the A-DALEC model, a biogeochemical model of carbon cycling in forests, which runs at an annual time step (see Additional file 1 A for full details) [15, 21].  $N_i^t$  and  $N_i^{t+1}$  are based on observed pixel uncertainty in SAR biomass estimates [13]. We



cannot base  $Bs_i^t$  directly on the observed biomass  $O_i^t$ , as the observation noise  $N_i^t$  cannot be determined (and thus removed) for each pixel, and so the A-DALEC model is used to spin-up an estimate of  $Bs_i^t$ , see Additional file 1 section B for full details. The equations above assume that  $t = 1$  and  $t = 2$  are separated by 1 year. When the separation is more than 1 year, as in the case of our OSSE, the base  $Bs_i^t$  should have the annual growth and disturbance applied once for each year of separation.

95 % confidence intervals for the factors  $E_p$  and  $E_l$  are found using a maximum likelihood estimation routine, see Additional file 1 C for full details. This routine finds the most likely combinations of  $E_p$  and  $E_l$  based on minimising the differences between the observed and simulated ensemble distributions;  $\Delta O = O^{t+1} - O^t$  and  $\Delta Os = Os^{t+1} - Os^t$ .

### Testing the framework parameter estimates

To allow the technique to be assessed against a known 'truth' we use a set of observation system simulation experiment (OSSE). In the OSSE we simulate two successive (noisy) biomass observations which have observation noise and a definable disturbance regime applied. The OSSE observations are derived by spinning up the A-DALEC model to match ALOS observations within the Gorongosa and Nhamatanda districts of Sofala province in central Mozambique. The area is dominated by dry miombo woodland, the dominant woodland type in Southern Africa, see Additional file 1 B. The first OSSE observation,  $t = 1$ , is taken at the end of the 1st year, the second observation,  $t = 2$ , is taken at the end of the 5th year, i.e. separated by 4 years. Separate spin-ups are performed for the  $\Delta O$  and  $\Delta S$  simulations. Three tests are performed; the first to assess the ability of the approach to identify  $E_M$ ,  $E_l$  and  $E_p$ , the second to assess the impact of observation bias and the third to determine impact of ensemble size.

### Determining the accuracy of the framework parameter estimates: test 1

A set of nine analyses were used to test the ability of our approach to identify  $E_M$ ,  $E_l$  and  $E_p$ . Each analysis was performed for the same size ensemble of  $n = 1600$  pixels, which equates to an area of 1000 by 1000 m given the 25 by 25 m pixel size of the ALOS biomass maps [13]. We perform OSSEs with four levels of mean disturbance  $E_M = 0, 0.018, 0.045, 0.090$  and  $0.180$ . These disturbance fractions equate to annual biomass loss rates of 0, 1.8, 4.5, 9 and 18 %. For each nonzero  $E_M$  we simulate a high intensity ( $E_l \gg E_p$ ) and low intensity ( $E_l \ll E_p$ ) disturbance scenario. In the high intensity cases only a few pixels are disturbed, but when disturbed 90 % of the biomass is lost (i.e.  $E_l = 0.9$ ). In the low intensity cases, 90 % of the

pixels are disturbed (i.e.  $E_p = 0.9$ ), but each disturbance results in a small loss of biomass at the pixel level. The various combinations of factors are shown in Table 1.

### Determining the impact of observation bias on the framework parameter estimates: test 2

To simulate the impact of observation bias we perturb the synthetic experiments using the bias observed in the actual biomass maps [13]. Only the first biomass observation (i.e. at time  $t = 1$ ) is biased by  $-160, 0$ , and  $160 \text{ gC m}^{-2}$ . The impact of the bias is assessed using both a low intensity case (i.e.  $E_l = 0.05$  and  $E_p = 0.9$ ), and a high intensity case (i.e.  $E_l = 0.9$  and  $E_p = 0.05$ ). In both cases the OSSE has an  $E_M = 0.045$  and an ensemble size of  $n = 1600$  pixels.

### Determining the impact of ensemble size on the framework parameter estimates: test 3

The impact of varying the ensemble size is tested for  $n = 6400, 1600, 400$ , and  $100$ . These ensembles equate to areas of 2000 by 2000 m (6400 pixels), 1000 by 1000 m (1600 pixels), 500 by 500 m (400 pixels), and 250 by 250 m (100 pixels). The areas are centred on the same location. We analyse these areas for a single low intensity disturbance regime  $E_M = 0.045$ ,  $E_l = 0.05$  and  $E_p = 0.9$ .

### Additional file

**Additional file 1.** A framework for estimating forest disturbance intensity from remotely sensed biomass maps: moving beyond average biomass loss estimates.

### Authors' contributions

The study was designed by all authors. TH performed the analysis and produced the figures and tables and wrote the manuscript. All co-authors contributed substantially to the interpretation of results and revision of the manuscript. All authors read and approved the final manuscript.

### Author details

<sup>1</sup> Department of Earth and Environmental Science, University of St Andrews, Irvine Building, North Street, St Andrews, UK. <sup>2</sup> School of GeoSciences, The University of Edinburgh, Edinburgh, UK. <sup>3</sup> The NERC National Centre for Earth Observation, St Andrews, UK.

### Acknowledgements

This work was funded by ESA (Contract No 4000102042/10/NL/CT), the NERC National Centre for Earth Observation, the NERC CarbonFusion project (NE/D000874/1), the Mpingo Conservation and Development Initiative and the EU Framework 7 I-REDD + project. ESA and JAXA provided the ALOS PALSAR imagery through C1P7493 and the 4th Research Agreement for the Advanced Land Observing Satellite-2. The authors would like to thank Klaus Scipal and Shaun Quegan for advice during the study. Finally we would like to thank the three anonymous reviewers for their helpful comments.

### Competing interests

The authors declare that they have no competing interests.

Received: 28 August 2015 Accepted: 27 October 2015

Published online: 02 December 2015

## References

1. FAO. Global forest resources assessment 2010: main report. FAO forestry paper. Rome: Food and agriculture organization of the United Nations; 2010. p. 2010.
2. Pan Y, Birdsey RA, Fang J, Houghton R, Kauppi PE, Kurz WA, et al. A large and persistent carbon sink in the world's forests. *Science*. 2011;333(6045):988–93. doi:[10.1126/science.1201609](https://doi.org/10.1126/science.1201609).
3. Achard F, Beuchle R, Mayaux P, Stibig H-J, Bodart C, Brink A, et al. Determination of tropical deforestation rates and related carbon losses from 1990 to 2010. *Glob Chang Biol*. 2014;20(8):2540–54. doi:[10.1111/gcb.12605](https://doi.org/10.1111/gcb.12605).
4. Hansen MC, Stehman SV, Potapov PV. Quantification of global gross forest cover loss. *Proc Natl Acad Sci USA*. 2010;107(19):8650–5. doi:[10.1073/pnas.0912668107](https://doi.org/10.1073/pnas.0912668107).
5. Mertz O, Müller D, Sikor T, Hett C, Heinimann A, Castella J-C, et al. The forgotten D: challenges of addressing forest degradation in complex mosaic landscapes under REDD+. *Geografisk Tidsskrift-Danish J Geogr*. 2012;112(1):63–76. doi:[10.1080/00167223.2012.709678](https://doi.org/10.1080/00167223.2012.709678).
6. Grime JP. Evidence for existence of three primary strategies in plants and its relevance to ecological and evolutionary theory. *Am Nat*. 1977;111(982):1169–94. doi:[10.1086/283244](https://doi.org/10.1086/283244).
7. Agarwal DK, Silander JA Jr, Gelfand AE, Dewar RE, Mickelson JG Jr. Tropical deforestation in Madagascar: analysis using hierarchical, spatially explicit, Bayesian regression models. *Ecol Model*. 2005;185(1):105–31. doi:[10.1016/j.ecolmodel.2004.11.023](https://doi.org/10.1016/j.ecolmodel.2004.11.023).
8. Ryan CM, Berry NJ, Joshi N. Quantifying the causes of deforestation and degradation and creating transparent REDD + baselines: a method and case study from central Mozambique. *Appl Geogr*. 2014;53:45–54. doi:[10.1016/j.apgeog.2014.05.014](https://doi.org/10.1016/j.apgeog.2014.05.014).
9. Herold M, Roman-Cuesta RM, Mollicone D, Hirata Y, Van Laake P, Asner GP, et al. Options for monitoring and estimating historical carbon emissions from forest degradation in the context of REDD+. *Carbon Balance Manag*. 2011;6(1):13. doi:[10.1186/1750-0680-6-13](https://doi.org/10.1186/1750-0680-6-13).
10. Hill TC, Williams M, Bloom AA, Mitchard ETA, Ryan CM. Are inventory based and remotely sensed above-ground biomass estimates consistent? *PLoS One*. 2013;8(9):e74170. doi:[10.1371/journal.pone.0074170](https://doi.org/10.1371/journal.pone.0074170).
11. Woodhouse IH, Mitchard ETA, Broily M, Maniatis D, Ryan CM. Radar backscatter is not a 'direct measure' of forest biomass. *Nature Clim Chang*. 2012;2(8):556–7.
12. Saatchi S, Ulander L, Williams M, Quegan S, LeToan T, Shugart H, et al. Forest biomass and the science of inventory from space. *Nature Clim Chang*. 2012;2(12):826–7.
13. Ryan CM, Hill TC, Woollen E, Ghee C, Mitchard E, Cassells G, et al. Quantifying small-scale deforestation and forest degradation in African woodlands using radar imagery. *Glob Chang Biol*. 2012;18:243–57. doi:[10.1111/j.1365-2486.2011.02551.x](https://doi.org/10.1111/j.1365-2486.2011.02551.x).
14. Le Toan T, Quegan S, Davidson MWJ, Balzter H, Paillou P, Papathanassiou K, et al. The BIOMASS mission: mapping global forest biomass to better understand the terrestrial carbon cycle. *Remote Sens Environ*. 2011;115(11):2850–60. doi:[10.1016/j.rse.2011.03.020](https://doi.org/10.1016/j.rse.2011.03.020).
15. Williams M, Hill TC, Ryan CM. Using biomass distributions to determine probability and intensity of tropical forest disturbance. *Plant Ecol Divers*. 2013;6(1):1–13. doi:[10.1080/17550874.2012.692404](https://doi.org/10.1080/17550874.2012.692404).
16. Harris NL, Brown S, Hagen SC, Saatchi SS, Petrova S, Salas W, et al. Baseline map of carbon emissions from deforestation in tropical regions. *Science*. 2012;336(6088):1573–6. doi:[10.1126/science.1217962](https://doi.org/10.1126/science.1217962).
17. Mitchard ETA, Saatchi SS, Woodhouse IH, Nangendo G, Ribeiro NS, Williams M et al. Using satellite radar backscatter to predict above-ground woody biomass: a consistent relationship across four different African landscapes. *Geophys Res Lett*. 2009;36. doi:[10.1029/2009GL040692](https://doi.org/10.1029/2009GL040692).
18. Williams M, Ryan CM, Rees RM, Sarnbane E, Fernando J, Grace J. Carbon sequestration and biodiversity of re-growing miombo woodlands in Mozambique. *For Ecol Manage*. 2008;254(2):145–55. doi:[10.1016/j.foreco.2007.07.033](https://doi.org/10.1016/j.foreco.2007.07.033).
19. Froliking S, Palace MW, Clark DB, Chambers JQ, Shugart HH, Hurtt GC. Forest disturbance and recovery: a general review in the context of space-borne remote sensing of impacts on aboveground biomass and canopy structure. *J Geophys Res Biogeosci*. 2009;114. doi:[10.1029/2008jg000911](https://doi.org/10.1029/2008jg000911).
20. Williams M, Hill TC, Ryan CM, Peylin P. Final report BIOMASS level 2 product to flux study. ESA contract No 4000102042/10/NL/CT. Noordwijk: The European Space Research and Technology Centre; 2011.
21. Williams M, Schwarz PA, Law BE, Irvine J, Kurpius MR. An improved analysis of forest carbon dynamics using data assimilation. *Glob Chang Biol*. 2005;11(1):89–105.

**Submit your manuscript to a SpringerOpen<sup>®</sup> journal and benefit from:**

- Convenient online submission
- Rigorous peer review
- Immediate publication on acceptance
- Open access: articles freely available online
- High visibility within the field
- Retaining the copyright to your article

---

Submit your next manuscript at ► [springeropen.com](http://springeropen.com)

---